Applied Thermal Engineering 162 (2019) 114264

Contents lists available at ScienceDirect

Applied Thermal Engineering

journal homepage: www.elsevier.com/locate/apthermeng

Experimental study on heat transfer characteristics of interior walls under partial-space heating mode in hot summer and cold winter zone in China

Li Nan[a,b], Chen Qiong[a,b,*]

[a] National Centre for International Research of Low-carbon and Green Buildings, Ministry of Science & Technology, Chongqing University, Chongqing 400045, China
[b] Joint International Research Laboratory of Green Buildings and Built Environments, Ministry of Education, Chongqing University, Chongqing 400045, China

HIGHLIGHTS

- Heat transfer characteristics of interior walls in south china has been studied.
- Heat transfer between adjacent rooms is studied under different heating terminals.
- Heat transfer between adjacent rooms increase heat load greatly.
- Heat transfer through inner walls affect energy consumption greatly.

ARTICLE INFO

Keywords:
Heat transfer between adjacent chambers
Intermittent heating
Thermal characteristics
Interior walls
Indoor thermal environment

ABSTRACT

In this paper, in order to study the effect of heat transfer between households on good indoor thermal environment and building energy efficiency, the indoor thermal environment and heat consumption of the room with different laying forms of radiation end are compared in the case of no heating in the adjacent room through the field experimental test. It was found that whether the adjacent room is heated directly affects the surface temperature and total heat consumption of the inner wall. Compared with the heating adjacent room, when the adjacent room is not heated the indoor air temperature in the working area decreased by 3.4-4.7%, the internal wall surface temperature decreased by 3.0–7.4%, and the heat flux density of internal wall surface increased by 29.8–52.2%. The heating surface temperature was reduced by 2.3–3.7%, the heat flux density of the heating surface was increased by 15.3–16.3% for floor and ceiling heating, and the heat flux density was reduced by about 22% because of the large heat transfer to adjacent rooms through interior walls. The heating of the large heat transfer to the adjacent rooms through interior walls. The total heat supply to the room increased by 5.2–7.2%. Additional heat load calculation is supposed to be taken into consideration due to the large heat transfer between interior walls while neighboring rooms are not heated.

1. Introduction

In the air conditioning load of the building, it has been agreed that the building envelope has a great influence on the indoor temperature and building heat load as well [1]. The solar radiation and the outdoor air pass through the heat transfer with the external enclosure to cause fluctuations in the indoor air temperature, and heat exchange is carried out through the inner envelope structure due to the existence of the temperature difference between adjacent rooms [2]. Therefore, studying the influence of the inner and outer envelope structures of buildings on indoor air temperature is of great significance to energy conservation.

In the hot summer and cold winter regions of China, the average outdoor temperature in the coldest winter months is below 10°, and the indoor thermal environment is poor. Unlike central heating in cold regions, the indoor air temperature resulted by users in the area adjusting the room temperature individually according to their own comfort, will get higher even in the case where the adjacent room is not heated. Then, the ratio of heat transfer between households through the internal envelope structure of the building to the total indoor heat load cannot be ignored. The heat transfer between the households causes the indoor air temperature to fail to meet the requirements and increase the energy consumption. Both the indoor thermal environment and energy efficiency suffer a negative impact.

At present, scholars at home and abroad have studied the external envelope structure and the inner envelope structure. Among them, the

* Corresponding author.
E-mail address: cq_505@163.com (Q. Chen).

https://doi.org/10.1016/j.applthermaleng.2019.114264
Received 9 March 2019; Received in revised form 2 July 2019; Accepted 15 August 2019
Available online 16 August 2019
1359-4311/ © 2019 Elsevier Ltd. All rights reserved.

research on the thickness, insulation and materials of the outer protective structure is becoming more and more mature [3]. In Europe and the United States, the internal insulation system is relatively perfect, so even if there is heat transfer in the adjacent chamber, it is usually not considered in the study [4]. In the area where the insulation structure has not yet reached the mature stage, it is necessary to consider the influence of the heat transfer between the adjacent rooms in the heat transfer calculation of the envelope structure.

In the process of studying the thermal properties of exterior walls with different orientations and different insulation layers, Tugce Pekdogan et al. numerically calculated the heat flux of the exterior walls through the one-dimensional transient heat equation using the finite difference method. The results showed that the insulation layers in the middle of the exterior walls resulted in more heat loss in the building. The insulation layers with thickness of 0.15 and 0.25 m in the middle of the exterior walls can save 65% (in summer) and 80% (in winter) compared to the TS825 at most which refers to Thermal Insulation Requirements for Buildings in Turkey [5].

Besides, there are also many researches focusing on influence of insulation thickness of building walls on energy saving. Naouel Daouas analyzed the building energy consumption and investment payback period based on the finite Fourier transform method to accurately calculate the annual cooling and heating load of the building to determine the optimal insulation thickness of the wall. The results showed that the optimal thickness of the insulation layer in the south-facing wall was 10.1 cm, the energy saving rate was 71.33%, and the investment recovery period was only 3.29 years, achieving the best economic effect comparing with buildings at other orientations [6].

Modeste Kameni Nematchoua et al. reviewed the study on building exterior walls insulation in Cameroon. Based on the life cycle model, the thickness, energy consumption and investment payback period of the insulation materials in a case were analyzed. Two typical wall structures (concrete block (HCB) and compression stabilized earth block wall (CSEB)) were investigated in this study. The results showed that the best insulation thickness for the south-facing wall was 0.09 m which can realized 79.80% of energy saving rate at least and the payback period was up to 4.73 years. The optimum insulation thickness of the HCB wall (0.0983 m) was higher than the CSEB wall (0.0958 m), while the HCB wall had a smaller payback period [8].

In addition, there are a lot of studies discussing the effect of location of insulation layer of building walls on indoor thermal environment. Meral Ozel studied the dynamic thermal properties of the wall using the finite difference element method. The results showed that the location of the insulation layer had a significant impact on the time lag factor and the reduction factor of the wall. The results of the analysis of the life expectancy of the building indicated that the heat load of walls and the optimal thickness of insulation layer were affected by the location of the insulation layer in the wall, and the external insulation caused smaller indoor temperature fluctuations and temperature peaks than that resulting of the intermediate insulation [7].

Furthermore, the heat transfer performance of the building wall is not only related to the thickness of the envelope structure, the material and the insulation layer. In fact, the coupling of these physical parameters will have a great impact on the overall performance of the wall. Jihui Yuan et al. proposed to come with the best combination values of surface reflectivity and thermal insulation thickness of exterior walls on the basis of the construction cost and heat load in six typical cities of Japan. By simulating the heat load of the exterior walls with a thickness of 10–100 mm and a surface reflectance of 0.1–0.8, the cost analysis method was used to determine the optimal combination values of surface reflectivity and thickness of the insulation layer, providing reference for the building envelope structure design [10].

Francesco Leccese et al. analyzed and predicted the dynamic thermal characteristics of interior and exterior walls using matrix heat transfer model, which is similar to a two-dimensional heat conduction model of an embedded building envelope proposed by Vadim Mizonov et al. describing the thermal process inside the building envelope in the form of a cyclic matrix [9]. The experimental results showed the relationship between the thickness and location of the insulation layer and the dynamic thermal properties of the wall, which characterized by dynamic heat transmission, reduction factor and time lag. In the premise of correcting the change of heat transfer of the external wall, the influence of the interior wall and floor on the indoor environment of the building was analyzed. It provided a reference for the design of building envelopes [11].

In addition, Dionysios I. Kolaitis [12] K.J. Kontoleon [13] Pan, Dongmei [14] L.Y. Zhang [15] and Xi Meng [16] et al. have studied the thermal properties and dynamic thermal response of the building structure, of which the research factors involved include wall type [17,18], wall material [19,20], thickness and configuration of the insulation layer [21–23].

In general, for non-centralized heating areas, there is a general uncertainty about the lack of heating and heating time in the adjacent areas, and the study of the heat transfer between the adjacent rooms on energy consumption and indoor thermal environment is relatively scarce. There are few studies on the influence of heating methods on the heat transfer process of the interior wall, and the transient process research is more lacking. However, in the case of diversified heating modes in the hot summer and cold winter regions, the influence of heating methods on the heat transfer of the interior wall is studied, which is the basis for the adaptive design of the interior wall and heating method, so there is still research space in this part. In this paper, the effects of heat transfer between the adjacent rooms under different heating methods (including floor heating, ceiling heating and wall heating) on the indoor thermal environment and energy consumption of the heating room are studied experimentally. The paper study the effect of heat transfers between adjacent rooms on building energy efficiency and provide the reference for the building heat load calculation and design of building envelop structures in hot summer and cold winter areas in China.

2. Heat transfer process

2.1. Thermal resistance and heat transfer coefficient

When studying the thermal resistance and heat transfer coefficient of the envelope structure, it is mainly for the steady-state heat transfer process. In practical engineering, the envelope is usually composed of a variety of materials. In addition, there is a composite flat wall, which is composed of different materials along the width and thickness, such as empty bucket wall, empty bucket wall, hollow panel and sandwich panel. There are two-dimensional or three-dimensional temperature fields on the common envelope structure in this type of engineering due to the different thermal conductivity of different materials. However, for the sake of simplicity, when the thermal conductivity of each material is not much different, it can be treated approximately as a one-dimensional heat conduction problem, and the one-dimensional heat transfer process of the envelope structure is shown in Fig. 1.

The heat transfer performance of the envelope structure is related to the material thickness d and the thermal conductivity coefficient λ of the material. The convective heat transfer coefficients h of the internal and external surfaces are inversely proportional to d, which is proportional to λ and proportional to h.

2.2. Heat storage coefficient

When the thickness of the enclosure is much smaller than its length and height, the enclosure can be considered a uniform semi-infinite wall. The surface heat storage coefficient of the envelope structure (Y) is equal to the heat storage coefficient of the material (S), which means that in the case of periodic heat disturbance, the heat flow for heating the surface of the enclosure is consumed by the surface temperature of

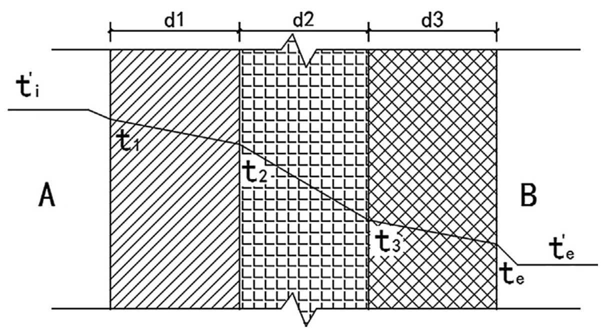

Fig. 1. One-dimensional heat transfer process of the envelope structure.

the enclosure being increased by 1 °C. When the thickness of the envelope is not large, Y is related to the thickness of the envelope material and the heat transfer between the internal and external walls, and S is only related to the nature of the material itself. Under the cyclical thermal disturbance, the heat storage coefficient of the material can indicate the degree of response when subjected to thermal disturbance.

When the thickness of the envelope structure is not much smaller than its length and height, that is, it cannot be regarded as an infinite wall. Because the surface temperature fluctuation of the external wall is also related to the boundary conditions in contact at this time, the heat storage coefficient of the surface of the material layer can be solved by the following method.

When the envelope structure is composed of multiple layers of material, a layer-by-layer calculation is required calculating the heat storage coefficient of the surface.

The heat storage coefficient of the inner surface of the enclosure structure is only suitable for the temperature fluctuation when the inner side is subjected to thermal disturbance. When studying the temperature fluctuation of the back-wave surface of the enclosure structure, the thermal inertia index is often used.

3. Experimental program

3.1. Experiment platform

The experimental platform is located on the experimental building of the School of Urban Construction and Environmental Engineering of Chongqing University. Three rooms of Room A, Room B and Room C are used in the experiment, of which the room sizes are 6 m × 3.5 m × 3.2 m (L × W × H), 6 m × 3.5 m × 3.2 m (L × W × H), and 6 m × 5 m × 3.2 m (L × W × H). The floor plan is shown in Fig. 2.

For convenience of description, the numbers of the room and its

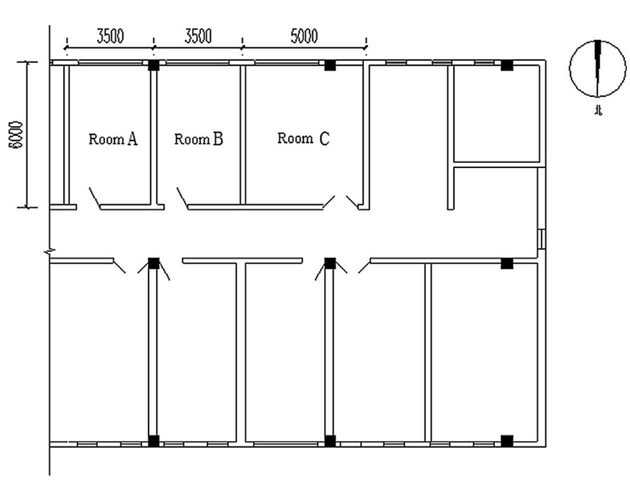

Fig. 2. Floor plan of the experimental room.

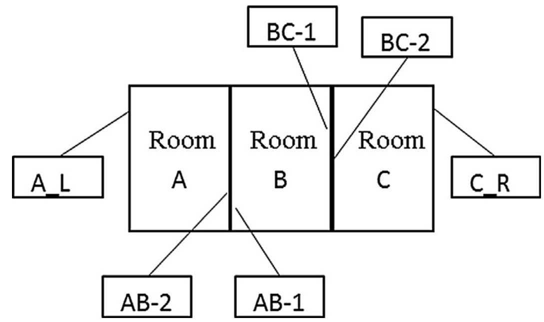

Fig. 3. Number of laboratory room and interior wall.

walls are shown in the Fig. 3, that is, the left and right walls of Room A are numbered A_L and AB_2, and the left and right walls of Room B are numbered AB_1 and BC_1. The left and right walls of Room C are numbered BC_1 and C_R. The heating ends involved in the experiment include the capillary in the left and right wall of room A, the floor capillary of room B, the wall coil of room B, the ceiling capillary of room B, and the capillary in left and right wall of room C. And the parameters of the enclosure structure of the experimental room are shown in Table 1.

3.2. Experimental scheme

In the case of the floor radiant heating, ceiling radiant heating, and wall radiant heating, the indoor thermal environment and heat supply of the room B and the thermal characteristics of the interior wall are compared when the neighboring rooms A and C are under the conditions of heating and natural temperature. The experimental conditions are shown in Table 2.

The experiment lasted for 12 h for all conditions, and Case 1 is repeated once in order to avoid the influence of outdoor temperature. In order to eliminate the influence of intermittent time on the heat flux density, each working condition is continuously operated for 12 h from the initial state, and there is no start-stop control.

In each case, the test parameters include:

(a) Outdoor air temperature, supply and return water temperature, flow rate, and heat supply;
(b) Floor surface temperature, interior and exterior surface temperatures of walls and windows, indoor air temperature;
(c) The heat flux density on the floor surface of Room B, the heat flux density on the ceiling surface, the heat flux density on the surface of AB_1 and AB_2, and the heat flux density on the surface of BC_1 and BC_2.

The detailed information of the experimental instrument is shown in Table 3.

The 10 temperature measuring points arranged in the ceiling are in a "plum-shaped" distribution. The floor is arranged with 15 measuring points in a "plum-shaped" distribution. The measuring point of the wall temperature is "plum-shaped" distribution, a total of 18. Five measuring points were selected in the same height horizontal direction, showing a "plum blossom type" distribution. Each position was arranged at a height of 0.1 m, 0.6 m, 1.1 m, 1.7 m and 2.5 m, for a total of five. Therefore, a total of 25 measuring points is arranged in the indoor space of the room. In the arrangement of measuring points, the main consideration is 0.1 m for the height of the human ankle, 0.6 m for the height of the human knee, and also the height when the person lies flat on the bed, 1.1 m is the height of the head when the human body sits down, and 1.7 m is the height of the top of the head when human body standing. The layout of measuring points of experimental rooms is shown in Fig. 4.

Table 1
Parameters of the enclosure structure of the experimental room.

Envelope	Material	Heat transfer coefficient ($W/m^2 \bullet K$)	Thermal resistance ($m^2 \bullet K/W$)
Exterior wall	240 mm solid brick wall	2.03	0.492
Interior wall	180 mm solid brick wall	2.39	0.419
Floor	Precast concrete slab	2.20	0.454
Door	Single-layer wooden door	2.91	0.344
Window	Single-layer glass aluminum window	6.40	0.156

Table 2
Experimental condition list.

Case		Room A	Room B	Room C
Case 1	1-1-a	/	Floor	/
	1-2-a	A_L	Floor	C_R
	1-1-b	/	Floor	/
	1-2-b	A_L	Floor	C_R
Case 2	2-1	/	Ceiling	/
	2-2	A_L	Ceiling	C_R
Case 3	3-1	/	Wall	/
	3-2	A_L	Wall	C_R
Case 4		AB_2	/	BC_2

4. Analysis of experimental results

4.1. Natural room temperature of the adjacent room

The natural indoor air temperature of the room is related to the performance of the enclosure structure, whether the adjacent room is heated, the window to wall ratio, and the number of air changes. After the adjacent room was not heated and the wall was basically warmed up (long time from the last heating ended), the natural indoor air temperature of the experimental room (the window was slightly open to meet the habits of window ventilation in the hot summer and cold winter areas) was higher about 2.37 °C than The average outdoor air temperature. Table 4 shows the outdoor air temperature and the average indoor air temperature at the initial time under experimental conditions.

4.2. Floor heating

This section analyzes the experimental results of Case 1. In order to avoid the influence of outdoor air temperature on the experimental results, this working condition is repeated once under different outdoor air temperatures, so there are four experimental conditions at total, which can be divided into group A and group B.

The surface temperature of the floor is as shown in Fig. 5(a), and the surface temperatures of the floor in the two cases were similar. The reason why the overlap rate of the floor surface temperature of the group A in the initial stage was slightly lower was that it was affected by the heat storage of the floor in the early stage, but the two curves were basically coincident after the stabilization. The rise phase of the floor surface temperature experienced three stages of slow temperature rise - rapid temperature rise - and stabilized. After heating for about 7 h, the floor surface temperature was stable at about 24.41 °C and 24.98 °C, respectively, with a difference of 0.57 °C.

The average temperature of the inner surface AB_1 in the two sets of experiments is shown in Fig. 5(b). It can be seen whether the adjacent chamber was heated had an effect on the temperature rise rate and the stable temperature of the inner surface AB_1. In the group A operating condition (outdoor average air temperature was 8.98 °C), the steady-state temperature of the inner surface AB_1 under the operating condition 1-1-a was 1.02 °C lower than that under the operating condition 1-2-a on average. The initial temperatures of the two operating conditions were 13.83 °C and 13.89 °C, respectively, which were relatively similar. In the group B operating condition (outdoor average air temperature was 10.74 °C), the steady-state temperature of the inner surface AB_1 under the operating condition 1-1-a was 1.46 °C lower than that under the working condition 1–2-a on average. The initial temperatures were 13.98 °C and 14.42 °C, respectively, with a difference of −0.44 °C. Then, after removing the influence of the initial temperature, the average temperature difference of the inner surface AB_1 of the two working conditions at the end of the experiment was 1.02 °C, which was similar to the working condition of the group A. It can be considered that in the outdoor temperature range of 8.98–10.48 °C, when the rooms A and C were not heated, the stable temperature of the inner surface AB_1 was 1.02 °C lower than that of the rooms A and C with heating.

The average indoor air temperature of the working area in the two sets of experiments is shown in Fig. 5(c). It can be seen whether the adjacent room was heated had an effect on the temperature rise rate and the stable temperature of the indoor air temperature in the work area. In group A conditions (outdoor average air temperature was 8.98 °C), the average indoor air temperature in the working areas under operating conditions 1-1-a and 1-2-a was stable at 17.54 °C and 18.12 °C, respectively, with a difference of 0.58 °C. The initial temperatures of the two operating conditions were 13.97 °C and 13.86 °C, respectively, which were relatively similar. In group B conditions (outdoor average air temperature was 10.74 °C), the average indoor air temperature in the working areas under operating conditions 1-1-a and 1-2-a was stable at 18.24 °C and 18.90 °C, respectively, with a difference of 0.67 °C. The initial temperatures of the two operating conditions

Table 3
The detailed information of the experimental instrument.

Instrument	Type	Range	Accuracy
Heat meter	UH32-6.0	0–105 °C	± 0.01 °C
		$0.02m^3/h$–$2.0m^3/h$	± $0.001m^3/h$
		/	± 1kW·h
T-type thermocouple	/	−40∼+125 °C	0.004•|t|
Agilent data logger	Agilent 34972A	−200∼+350 °C	/
Temperature and humidity recorder HOBO	HOBO/UX100-011	Temperature: −20 to 70 °C	Temperature: ± 0.21 °C
		Relative humidity:1%∼95% RH	Relative humidity: ± 3.5%(25–85%), ± 2.5%(10–90%)
Thermal Imager	FLIR T650sc	−40 to 150 °C	1%
Flow meter data logger	DaqPRO 5300	Depending on the type of defined channel	/
Heat flux sensor	HS-30	± $200kW/m^2$	3%

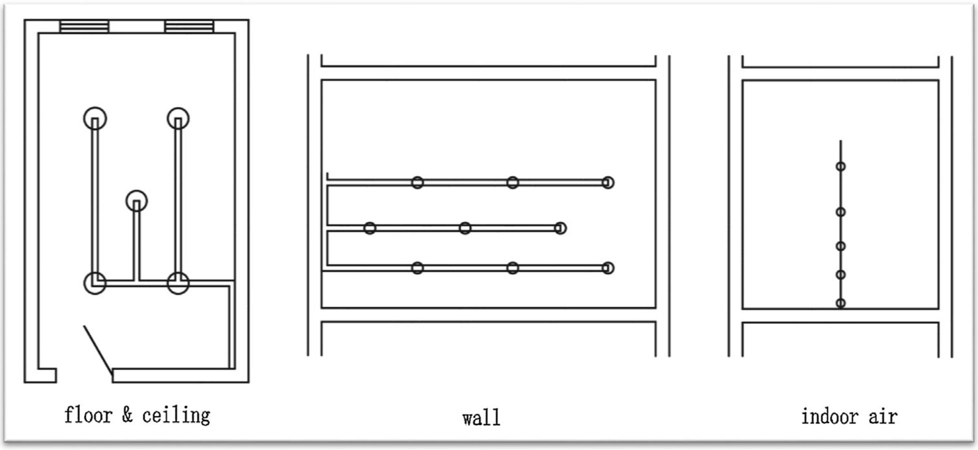

Fig. 4. The layout of measuring points of experimental rooms.

Table 4
Outdoor air temperature and the average indoor air temperature.

Outdoor air temperature (°C)	Natural indoor air temperature(°C)	Temperature difference (°C)
9.53	12.17	2.64
9.31	11.52	2.21
10.81	12.85	2.04
7.75	10.35	2.60

were 14.33 °C and 14.42 °C, respectively. It can be considered that in the outdoor temperature range of 8.98–10.48 °C, when the rooms A and C were not heated, the average indoor air temperature in the working area was 0.58–0.67 °C lower than that while the room A and C were heating.

Fig. 5(d) shows the heat flux density of the floor surface under the group B operating conditions (outdoor average air temperature was 10.48 °C). It can be seen that the heat flux density of the floor surface showed a trend of slow change-rapidly increasing-gradually stable with time under the two working conditions. The heat flux density on the floor surface tent to be stable after about 5.5–6 h of heating and whether the adjacent room was heated had an effect on the heat flux density. When the adjacent chambers A and C were heated, the heat flux density at the measuring point on the floor surface was about 58.10 W/m^2, and the heat flux density at the surface measurement point was about 49.97 W/m^2 while the adjacent chambers A and C were not heated, which was 8.13 W/m^2 lower than the former.

As shown in Fig. 5(e), the heat flux density on the surface of the inner wall surface AB_1 under the group B condition (outdoor average air temperature was 10.48 °C). Since only one heat flow sheet was arranged on the surface of AB_1, the measured value only represented the heat flux density value of the measuring point, not the average heat flux density of the wall surface AB_1. It showed that the heating of the adjacent room had a great influence on the heat flux density of the wall AB_1. The heat flux density of the wall AB_1 experienced a rapid increase and then a slow decrease, reaching a peak about 5.5 h after the start of heating. The peak heat flux density of the wall surface AB_1 while the adjacent rooms were at the natural indoor air temperature (condition 1-1-b) was 9.36 W/m^2, and finally stabilized at 7.49 W/m^2. When the neighboring rooms A and C were both heated (condition 1-2-b), the peak value was 6.15 W/m^2 and finally stabilizes at 4.95 W/m^2, which were 3.21 W/m^2 and 2.53 W/m^2 lower than the former respectively.

The total heat supply of the system to room B in each working condition under case 1 is shown in Table 5, which contains two parts: the heat storage of the floor and the heat released from the floor to the surrounding structure of the room and the air. The heat flux density at the center point of the floor surface does not represent the average heat flux density of the floor surface, so the measured value is not time integrated to determine the total heat released. The total heat supply to room B can be obtained by a heat meter. It can be seen from the above table whether the heating of the adjacent room had an influence on the total heat supply. According to 1-1-a and 1-2-a, when the outdoor average air temperature was 8.68 °C, the total heat supplied to room B when the adjacent rooms A and C were not heated was 5.021 MJ higher than that while the neighboring rooms A and C were heated. According to 1-1-b and 1-2-b, when the outdoor average air temperature was 10.73 °C, the total heat supplied to room B when the adjacent rooms A and C were not heated is 3.568 MJ higher than that while the neighboring rooms A and C were heated. That is, in the outdoor air temperature range of 8.98–10.48 °C, the total heat supply to room B when the adjacent rooms A and C were not heated is 3.568–5.021 MJ more than that when the adjacent rooms A and C were heated which was 4.6–6.9%.

4.3. Ceiling heating

This section analyzes the test results of case 2 which includes 2 conditions.

The inner surface temperature of the ceiling is shown in Fig. 6(a). Unlike floor heating, the smaller depth of the capillary inside the ceiling caused the inner surface temperature of the ceiling to rise rapidly from the start of heating and then tent to be stable after the heating began for about 3.5 h. The temperature curve of the inner surface of the ceiling under the two working conditions was close to coincident at the initial stage, and there were slight differences between the two curves in the steady state. The inner surface temperature of the ceiling under the working condition 2–1 in which the adjacent chambers A and C were not heated was stabilized at about 30.33 °C. The inner surface temperature of the ceiling under the working conditions 2–2 in which the adjacent rooms A and C were heated was about 31.50 °C, which was 1.17 °C higher than the former.

The average surface temperature of AB_1 is shown in Fig. 6(b). It can be seen that the surface temperature of AB_1 rise rapidly at the start of heating when the ceiling was heated, and then slowly rise to a stable level. Under the condition 2-1, when the adjacent chamber was not heated, the average surface temperature of AB_1 was 13.62 °C at the initial time, and then stabilized at 17.03 °C. When the adjacent room was under working condition 2-2, the average surface temperature of AB_1 was 13.73 °C at the initial time, and then stabilized at 18.40 °C, which was 1.37 °C higher than the former. Subtracting the influence of the temperature difference at the initial time, it was considered that the average surface temperature of AB_1 was reduced by 1.21 °C compared with the heating of the adjacent room due to the heat transfer of the

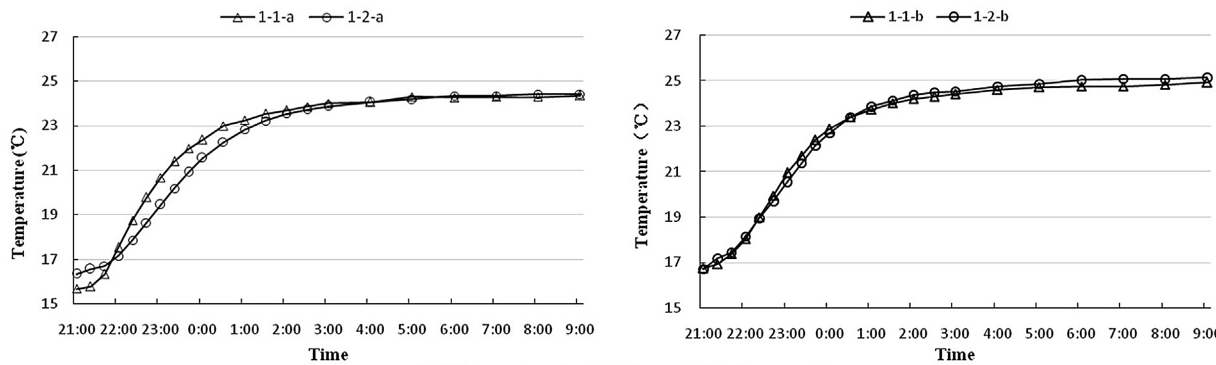

(a) The average temperature on the floor surface

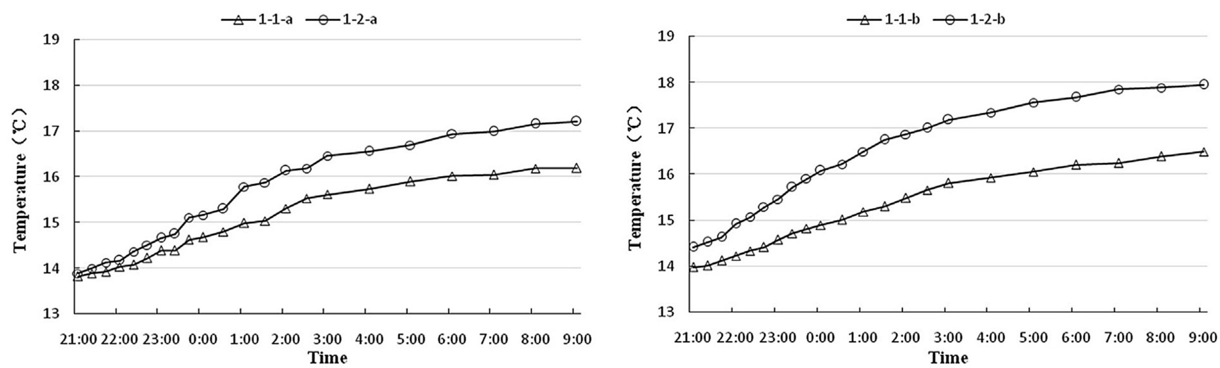

(b) The average surface temperature on AB_1

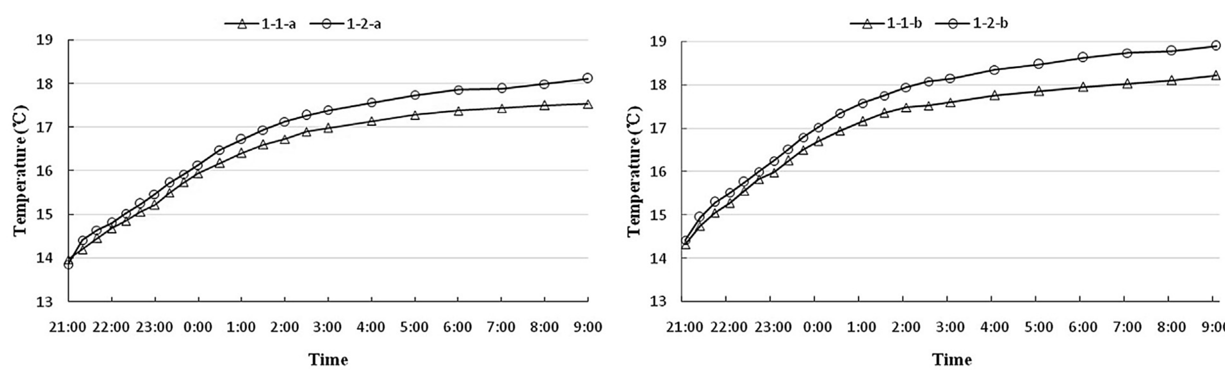

(c) The average temperature in the working area

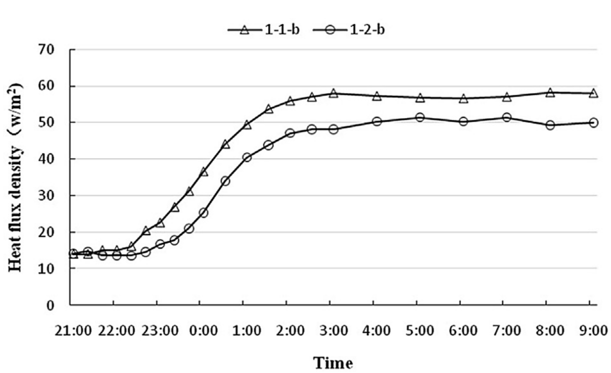

(d) The heat flux density of the measuring point on the floor

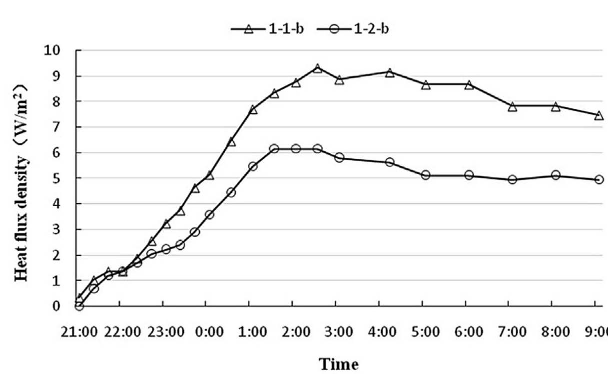

(e) The heat flux density of the measuring point on AB_1

Fig. 5. Experimental results for case 1.

non-heating adjacent chamber.

The average air temperature in the work area is shown in Fig. 6(c). It can be seen that the indoor air temperature of the ceiling heating was rapidly increased from the start of heating, which was different from the floor heating. Whether or not the adjacent room was heated had an effect on the average air temperature in the work area, especially during the period of stabilization. Under the condition 2-1 of no heating in the adjacent room, the average air temperature in the working area

Table 5
Total heat supply of Room B.

Case	Heat supplied to Room B (MJ)
1-1-a	72.396
1-2-a	67.375
1-1-b	78.048
1-2-b	74.480
2-1	78.119
2-2	74.235
3-1	80.784
3-2	75.348

was 13.76 °C, and tent to stable at 17.79 °C. Under the condition 2-2 of adjacent room heating, the initial average air temperature in the working area was 13.83 °C then reached 18.55 °C after 12 h. That is, the average air temperatures in the working area under the two working conditions were similar at the initial time. However, at the end time, the adjacent room heating conditions were relative to the adjacent room heating conditions, and the average air temperature in the working area while the adjacent rooms were not heated was 0.76 °C lower than of which the neighboring chambers were heated.

The heat flux density on the inner surface of the ceiling is shown in Fig. 6(d). It can be seen that the heat flux density of the inner surface of the ceiling under both working conditions showed a trend of slow change with time - rapid increase - gradually stable, and then tent to be stable after about 4.5–5 h of heating. After entering the stabilization phase, the heat flux density on the inner surface of the ceiling under the heating conditions of the adjacent rooms A and C was about 67.10 W/m^2, while the heat flux density at the inner surface of the ceiling under the non-heating conditions of the adjacent chambers A and C was about 58.18 W/m^2 which was 8.93 W/m^2 lower than the former.

The heat flux density on the inner wall surface AB_1 is shown in

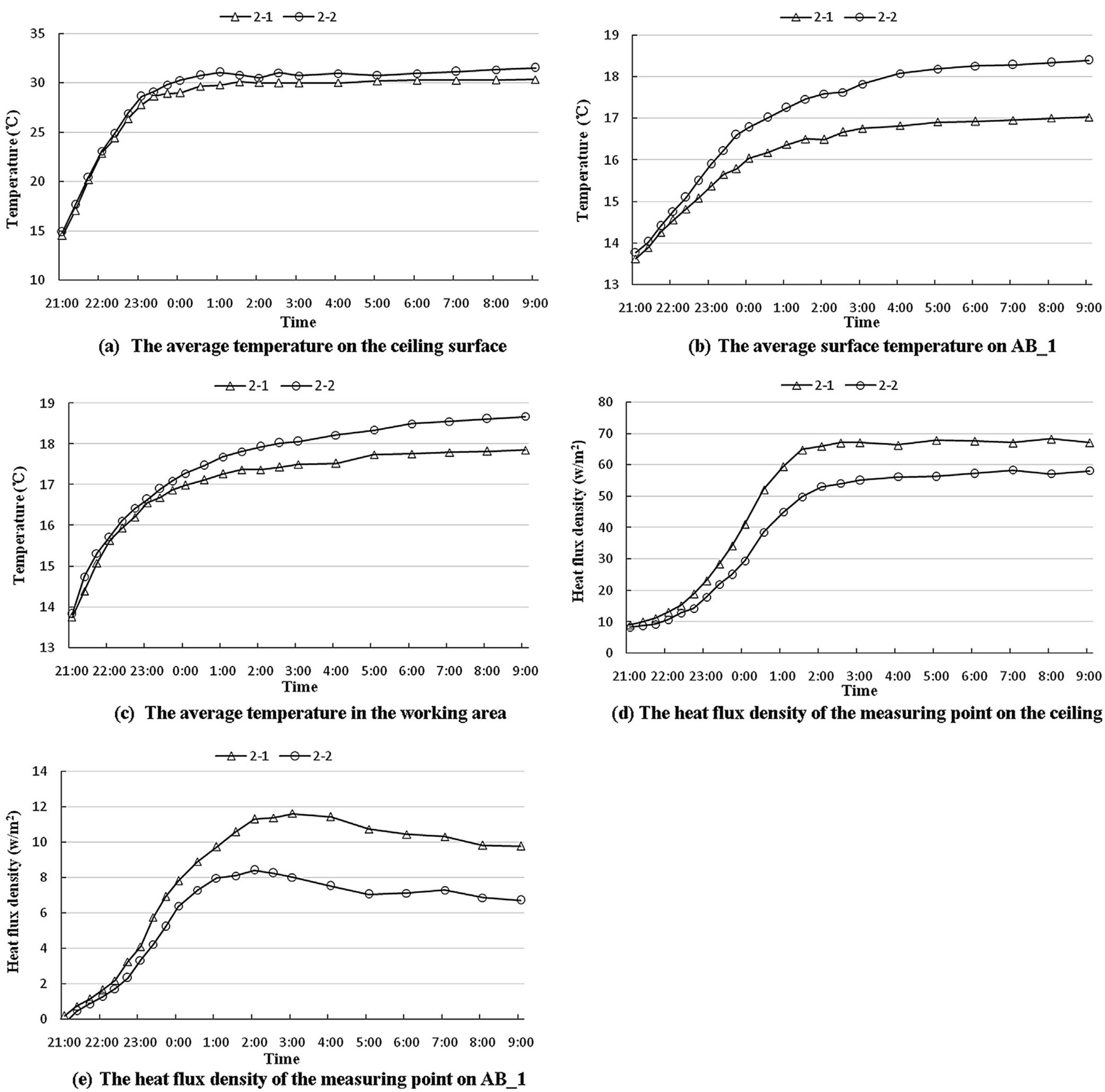

Fig. 6. Experimental results for case 2.

Table 6
The temperature increase and the peak heat flux density for case 1-3.

Case	Heating	Temperature increase in the working area (°C)	Temperature increase on AB_1 (°C)	Temperature increase on BC_1 (°C)	The peak heat flux density on AB_1 ($W/m^2 \cdot K$)	The peak heat flux density on BC_1($W/m^2 \cdot K$)
1-1(average)	Floor	3.74	2.44	2.25	9.36	8.95
1-2(average)		4.37	3.43	3.16	6.15	6.02
Difference		0.63	0.99	0.92	3.21	2.93
2-1	Ceiling	4.03	3.34	3.30	11.60	11.03
2-2		4.73	4.51	4.31	8.40	7.99
Difference		0.70	1.17	1.01	3.21	3.04
3-1	Wall	6.06	11.62	8.34	49.20	38.07
3-2		7.01	12.68	9.92	37.71	29.13
Difference		0.95	1.06	1.58	11.49	8.94

Fig. 6(e), which represents only the heat flux density of the measuring point, not the average heat flux density of the wall AB_1. It can be seen that the heat flux density of the wall AB_1 increased rapidly until the heating reaches a peak after about 5 h and began to slowly decrease. Under the natural indoor temperature of the adjacent room (condition 2-1) and the heating conditions of the adjacent rooms A and C (condition 2-2), the peak heat flux density of the inner wall AB_1 was 11.60 W/m^2 and 8.94 $W/\ m^2$ respectively, between which the difference was 3.06 W/m^2. The heat flux density of the inner wall surface AB_1 was 9.77 W/m^2 and 6.70 W/m^2 at the terminal time respectively, between which the difference was 3.21 W/m^2.

The total heat supply to the room under two conditions during continuous heating for 12 h is shown in Table 6, which consists of three parts: the heat storage of the ceiling, the heat transfer from the ceiling to the upper room and the heat released from the ceiling to the enclosure and air. Since the heat flux density at the inner surface of the ceiling does not represent the average heat flux density on the inner surface of the ceiling, the measured value is not time integrated to obtain the total heat released, which can be obtained from the heat meter. It can be seen from the table that the total heat supplied to the room B while the adjacent rooms A and C without the heating was 3.884 MJ more than that of the adjacent rooms A and C were heated, witnessing an increase of 5.0%.

4.4. Wall heating

This section analyzes the results of case 3 which contains two conditions when the wall heating system is on operation.

The average surface temperature of the inner surface AB_1 is as shown in Fig. 7(a). Since both the surfaces of AB_1 and the BC_1 were used for heating, only the AB_1 was taken for analysis. It can be seen that the surface temperature of AB_1 rise rapidly at the start of heating when the wall was heated, and tent to be stable after about 3 h. Under the condition 3-1 of the adjacent room with non-heating, the average surface temperature was 15.33 °C at the initial time and 26.95 °C at the end time. Under the condition 3-2 of the adjacent room with heating, the average surface temperature was 15.30 °C at the initial time and 27.98 °C at the end time, which was 1.03 °C lower than that of the former condition. Subtracting the influence of the temperature difference at the initial time, it can be considered that while the wall heating was on operation, the average temperature of the inner surface AB_1 was reduced by 1.06 °C with respect to that of which the adjacent room was heated due to the heat transfer of the non-heating adjacent chamber.

The average air temperature in the work area is shown in Fig. 7(b). It can be seen that the indoor air temperature under the wall heating rapidly rise from the start of heating, and then tent to be stable. Whether the adjacent room was heated or not had a significant effect on the temperature rise curve of the indoor air temperature. Under the condition of no heating in the adjacent room, the average air temperature in the working area was 13.51 °C at the initial time and 19.57 °C at the end time. Under the condition of heating in the adjacent room, the average air temperature in the working area was 13.52 °C at the initial time and 20.53 °C at the terminal time. Subtracting the influence of the initial temperature difference, the average air temperature in the working area while the neighboring rooms were not heated is 0.95 °C lower than that in which the adjacent rooms were heated.

The heat flow density of the measuring point on the inner wall surface AB_1 is as shown in Fig. 7(c). It can be seen that, unlike floor heating and ceiling heating, when the wall was heated, its heat flux density had experienced two stages of "rapid growth – tending to be stable". The measurement showed that the heat flux density of the wall surface tent to be stable after about 4.5–5 h from the heating, and whether the adjacent room was heated had a great influence on the growth rate and stable value of the heat flux density of the heating wall surfaces AB_1 and BC_1. When the neighboring room was not heated (3-1), the measured heat flow density of the wall AB_1 was about 48.08 W/m^2 in the stable phase. While the neighboring rooms A and C were both heated (3–2), the value was stable at 37.53 W/m^2, which was 10.55 W/m^2 lower than the former.

The heat flux density of the measuring point on the external surface AB_2 is as shown in Fig. 7(d). It can be seen that the wall AB_2 absorbed heat from the rooms A and B when the adjacent room was heated. When the adjacent room was not heated, the wall AB_2 that absorbed the heat from the room B releases heat, which was further hull to the room A. The heat flux density of AB_2 under the heating condition of adjacent room (3-2) showed a trend of increasing first and then decreasing slowly, of which the absolute value was about 15.06 W/m^2 at the end of the experiment. The heat flux density of the wall AB_2 under the non-heating condition of the adjacent room (3-1) continued to increase, of which the absolute value was 5.87 W/m^2 at the end time.

The total heat supply to room B for 12 h under both conditions is shown in Table 4 which can be obtained from the heat meter. It consists mainly of three parts: heat storage of the wall, heat transfer from the wall to room B, and heat transfer from the wall to the adjacent chamber. It can be seen that the compared with 3-2, and the total heating capacity of room B while neighboring rooms A and C were not under heating condition is 5.436 MJ, which was increased by 6.7% comparing with that of where the adjacent room A and C are heated.

4.5. Indoor thermal environment in non-heated neighborhoods

This section analyzes the experimental results of Condition 4 (wall AB_2 of adjacent room A and wall BC_2 of adjacent room C for heating).

The heating power to the room A (heat supply per unit time) is as shown in Fig. 8(a). It can be seen that different from the heat flux density of the wall AB_2 peaking at about 3.5 h, the total heat supply to the room A reached a top after about 1.5 h from heating, and then slowly decreased. The cause of the fluctuations and the heating system were related to the changing water supply temperature of the air-cooled heat pump system.

Under working condition 4 (the wallAB_2 on the right side of the

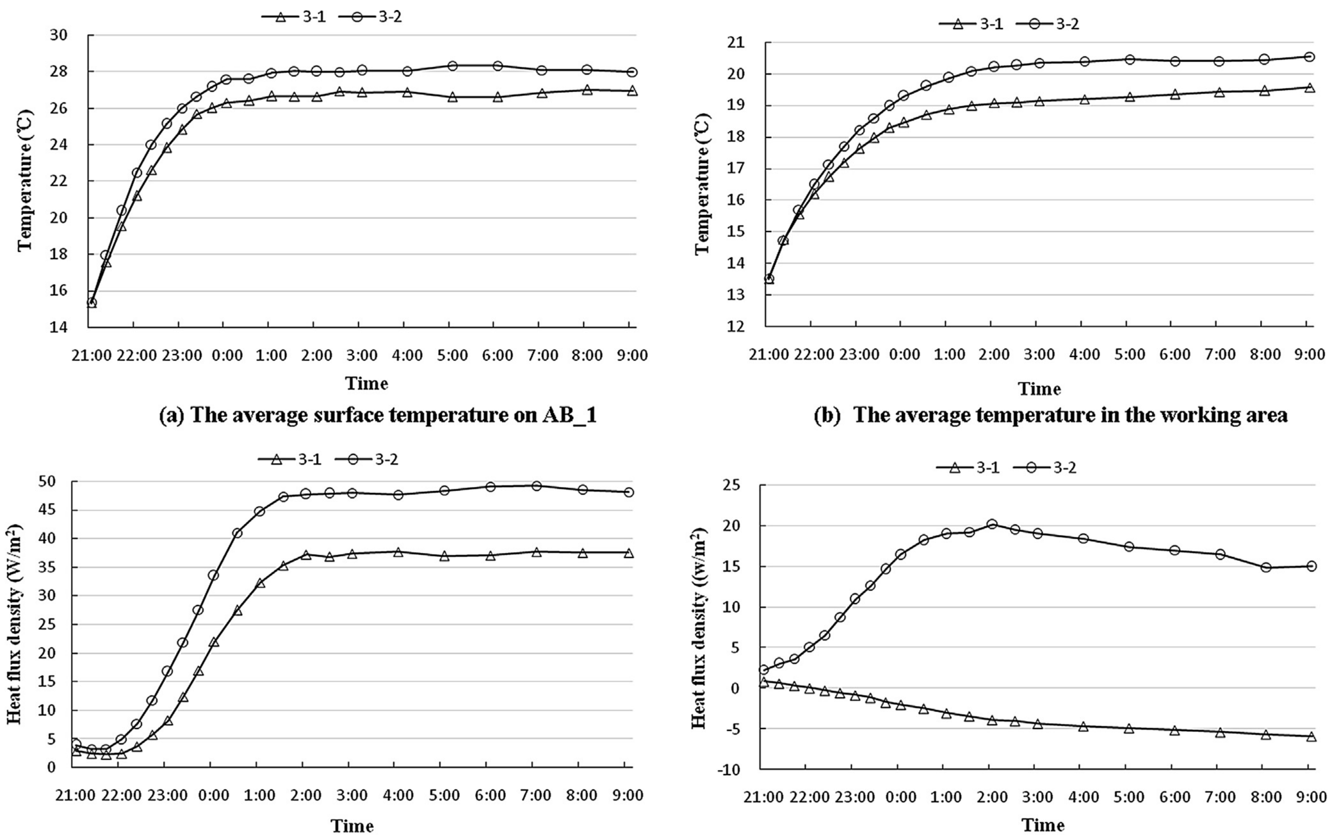

(a) The average surface temperature on AB_1

(b) The average temperature in the working area

(c) The heat flux density of the measuring point on AB_1

(d) The heat flux density of the measuring point on AB_2

Fig. 7. Experimental results for case 3.

room A and the wall BC_2 on the left side of the room C were heated, the room B was not heated) the temperature and heat flux density of the heating surface (AB_2 and BC_2) were shown in Fig. 8(b). It can be seen that the surface temperatures of the heating walls AB_2 and BC_2 rise rapidly at first, lasting for about 80 min, and then tent to be stable at about 31.61 °C (AB_2) and 32.60 °C (BC_2) respectively. However, the heat supplied to the wall rise rapidly after a slow rise of 20 min and then peaked after about 3.5–4 h. Then the heat supply tent to be gentle and slowly descends. The flow density of the two walls was about 116 W/m^2 at the terminal time. Further, with respect to the heat supply per unit time in Fig. 8(a), the small fluctuation of the measured heat flux density of the wall surface AB_2 was related to the heat storage and attenuation of the wall.

The average temperature of the inner surfaces AB_1 and BC_1 and the working area of the room B (0.1 m-1.7 m) within 24 h of adjacent room heating is shown in Fig. 8(c). Affected by the heat transfer of the wall, the surface temperatures of the inner walls AB_1 and BC_1 of the room B increased slowly for 4.5–5 h, and the temperature rise rate continued to increase. The reason was that when the rooms A and C just started heating, the two inner walls were in a state of heat storage, and the heat flow to the walls of the AB_1 and BC_1 began to increase significantly after about 4.5–5 h. The temperature rises of the inner surfaces AB_1 and BC_1 were 5.00 °C and 4.88 °C respectively during the 24 h period.

The average air temperature in the working area of room B was mainly affected by the heat transfer from the adjacent room, and also by the outdoor air temperature and the heat storage and release of each wall. The average air temperature in the working area of room B was slowly warmed up in the initial stage until 2:00 am, with a 0.5 h delay relative to the temperature changes of the walls AB_1 and BC_1. The average temperature of the work area of room B rise until10:00 the next day, then the heating rate increased again, which was affected by the outdoor temperature. After 16:00, the average air temperature rise rate in the room B working area became slower. Within 24 h of heating, the average air temperature in the working area of room B increased by 2.91 °C, which was 21% higher than its initial temperature.

The indoor air temperature of room B at different heights is shown in Fig. 8(d). It can be seen that the room air temperature in room B was evenly distributed due to the heating of the adjacent rooms on both sides, and generally showed a trend of decreasing from top to bottom.

Table 6 shows the temperature increase and the peak heat flux density under the conditions of Experiments 1–3. As a whole, whether or not the adjacent room had the greatest impact on the heating of the wall, followed by ceiling heating (ceiling laying) and floor heating (wood floor), for which the greater depth of the floor heating pipe and the heat capacity of the wooden floor were responsible. The surface temperature of the wood floor heating was lower than that of the ceiling and the wall heating, resulting in the heat released to the room and the indoor air temperature relatively small. The heating pipe for wall heating directly laid on the inner wall and the fact that both sides of the wall were heated in the experiment were the main reason why the heat transfer to the adjacent rooms and the total heat storage capacity of the wall were larger than that of the ceiling heating. Whether the room was heated or not had greater impact on the wall heating.

As illustrated in Table 7, when the adjacent rooms were not heated, the indoor air temperature in the working area decreased by 3.4–4.7%, the internal wall surface temperature decreased by 3.0–7.4%, and the heat flux density of internal wall surface increased by 29.8–52.2%. The heating surface temperature was reduced by 2.3–3.7%, the heat flux density of the heating surface was increased by 15.3–16.3% for floor and ceiling heating, and the heat flux density was reduced by about 22% because of the large heat transfer to adjacent rooms through interior walls. The heating of the large heat transfer to the adjacent rooms through interior walls. The total heat supply to the room increased by

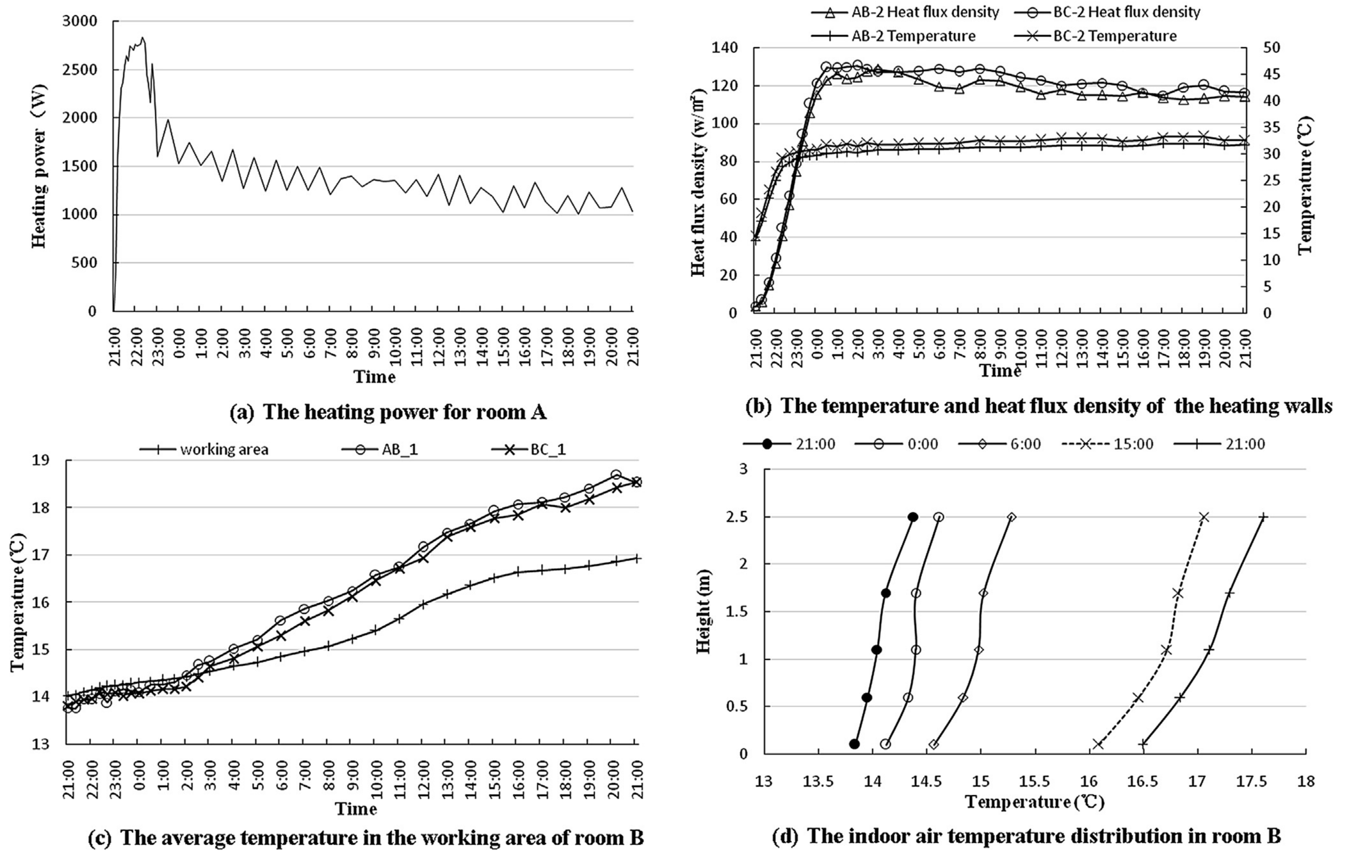

Fig. 8. Experimental results for case 4.

5.2–7.2%.

5. Conclusion

In this paper, under the three heating modes of floor radiant heating, ceiling radiant heating and wall radiant heating, the indoor thermal environment and heat flux density of heating room B while adjacent rooms A and C are under the heating and non-heating conditions are tested and analyzed. The following conclusions can be obtained.

(1) After the adjacent room is not heated and the heat of wall is released totally (the longer time from the last heating), the average temperature difference between the natural indoor air and the outdoor air is about 2.37 °C;
(2) The heating rate of the wall when the adjacent room is heated is greater than that where the adjacent room is not heated. The heat flux density of the heating surface changes rapidly and tends to be stable after 5.5–6 h (floor heating) and4.5–5 h (ceiling heating and wall heating).
(3) Considering the average air temperature in the working area and the surface temperature of each wall, whether the adjacent room are heated or not has the greatest influence on the wall heating, followed by the ceiling heating and floor heating.
(4) Within 24 h, the temperatures of the inner surfaces AB_1 and BC_1 of the neighboring room increased by 5.00 °C and 4.88 °C, respectively. The average air temperature in the working area of the non-heating room increased by 2.91 °C which was 21% higher than that at the initial time.
(5) Whether the adjacent rooms are heated or not causes the difference in the average air temperature in the working area is 0.62 °C (floor heating), 0.76 °C (ceiling heating), 0.95 °C (wall heating) which decrease by 3.4–4.7%.
(6) Whether the adjacent rooms are heated or not has the greatest

Table 7
The comparison of temperature, heat flux density and heat supply increase between case 1-3.

Case	Heating	Temperature in the working area (°C)	Temperature on AB_1 (°C)	Peak heat flux density on AB_1 (W/m^2)	Temperature on heating surface (°C)	Peak heat flux density on heating surface (W/m2)	Total heat supplies (MJ)
1-1(average)	Floor	17.89	16.71	9.36	24.41	58.10	75.222
1-2(average)		18.51	17.22	6.15	24.98	49.97	70.928
Increase ratio		−3.4%	−3.0%	52.2%	−2.3%	16.3%	6.1%
2-1	Ceiling	17.79	17.03	11.60	30.33	67.10	78.119
2-2		18.55	18.40	8.94	31.50	58.18	74.235
Increase ratio		−4.1%	−7.4%	29.8%	−3.7%	15.3%	5.2%
3–1	Wall	19.57	26.95		26.95	37.53	80.784
3–2		20.53	27.98		27.98	48.08	75.348
Increase ratio		−4.7%	−3.7%		−3.7%	−22.0%	7.2%

influence on the average temperature and the heat flow density of the inner wall surface. Under the two working conditions, the difference in the average inner surface temperature of the partition wall is: 1.02 °C (floor heating), 1.21 °C (ceiling heating), and 0.95 °C (wall heating) which reduce by 2.3–3.7%.

(7) The difference in peak heat flux density on the inner wall surface is 3.21 W/m^2 (floor heating), 3.06 W/m^2 (ceiling heating), and 10.55 W/m^2 (wall heating) which increased by 29.8–52.2%. The difference in total heat supply is: 4.30 MJ (floor heating), 3.88 MJ (ceiling heating), and 5.44 MJ (wall heating) which increase by 5.2–7.2%; Additional heat load calculation is supposed to be taken into consideration due to the large heat transfer between interior walls while neighboring rooms are not heated.

Acknowledgments

This research is supported by the China National Key R&D Program "Energy-saving design and key technical equipment development for clean air-conditioning plants" (Grant number 2018YFC0705206) and the Fundamental Research Funds for the Central Universities (Grant number 2018CDJDCH0015).

Appendix A. Supplementary material

Supplementary data to this article can be found online at https://doi.org/10.1016/j.applthermaleng.2019.114264.

References

[1] O. Kaynakli, A review of the economical and optimum thermal insulation thickness for building applications, Renew. Sustain. Energy Rev. 16 (1) (2012) 415–425, https://doi.org/10.1016/j.rser.2011.08.006.

[2] P. Ihm, L. Park, M. Krarti, D. Seo, Impact of window selection on the energy performance of residential buildings in South Korea, Energy Policy 44 (2012) 1–9, https://doi.org/10.1016/j.enpol.2011.08.046.

[3] M. Thalfeldt, J. Kurnitski, H. Voll, Detailed and simplified window model and opening effects on optimal window size and heating need, Energy Build. 127 (2016) 242–251, https://doi.org/10.1016/j.enbuild.2016.06.002.

[4] K. Tsikaloudaki, K. Laskos, T. Theodosiou, D. Bikas, The energy performance of windows in Mediterranean regions, Energy Build. 92 (2015) 180–187, https://doi.org/10.1016/j.enbuild.2015.01.059.

[5] T. Pekdogan, T. Basaran, Thermal performance of different exterior wall structures based on wall, Appl. Therm. Eng. 112 (2007) 15–24, https://doi.org/10.1016/j.applthermaleng.2016.10.068.

[6] N. Daouas, A study on optimum insulation thickness in walls and energy savings in Tunisian buildings based on analytical calculation of cooling and heating transmission loads, Appl. Energy 88 (1) (2011) 156–164, https://doi.org/10.1016/j.apenergy.2010.07.030.

[7] M. Ozel, Effect of insulation location on dynamic heat-transfer characteristics of building external walls and optimization of insulation thickness, Energy Build. 72 (2014) 288–295, https://doi.org/10.1016/j.enbuild.2013.11.015.

[8] M.K. Nematchoua, C.R. Raminosoa, R. Mamiharijaona, T. René, J.A. Orosa, W. Elvis, P. Meukam, Study of the economical and optimum thermal insulation thickness for buildings in a wet and hot tropical climate: case of Cameroon, Renew. Sustain. Energy Rev. 50 (2015) 1192–1202, https://doi.org/10.1016/j.rser.2015.05.066.

[9] V. Mizonov, N. Yelin, A. Sakharov, Theoretical study of the thermal state of building envelop in the, Appl. Therm. Eng. 79 (2015) 149–152, https://doi.org/10.1016/j.applthermaleng.2015.01.029.

[10] C.F. Jihui Yuan, Md. Kazuo Emura, Ashraful Alam, Proposal for optimum combination of reflectivity and insulation thickness of building exterior walls for annual thermal load in Japan, Build. Environ. 103 (2016) 228–237, https://doi.org/10.1016/j.buildenv.2016.04.019.

[11] G.S. Francesco Leccese, Francesco Asdrubali, Paola Gori, Passive thermal behaviour of buildings: Performance of external multilayered walls and influence of internal walls, Appl. Energy 225 (2018) 1078–1089, https://doi.org/10.1016/j.apenergy.2018.05.090.

[12] D.I. Kolaitis, E. Malliotakis, D.A. Kontogeorgos, I. Mandilaras, D.I. Katsourinis, M.A. Founti, Comparative assessment of internal and external thermal insulation systems for energy efficient retrofitting of residential buildings, Energy Build. 64 (2013) 123–131, https://doi.org/10.1016/j.enbuild.2013.04.004.

[13] K.J. Kontoleon, C. Giarma, Dynamic thermal response of building material layers in aspect of their moisture content, Appl. Energy 170 (2016) 76–91, https://doi.org/10.1016/j.apenergy.2016.01.106.

[14] D. Pan, M. Chan, S. Deng, Z. Lin, The effects of external wall insulation thickness on annual cooling and heating energy uses under different climates, Appl. Energy 97 (2012) 313–318, https://doi.org/10.1016/j.apenergy.2011.12.009.

[15] L.Y. Zhang, L.W. Jin, Z.N. Wang, J.Y. Zhang, X. Liu, L.H. Zhang, Effects of wall configuration on building energy performance subject to different climatic zones of China, Appl. Energy 185 (2017) 1565–1573, https://doi.org/10.1016/j.apenergy.2015.10.086.

[16] X. Meng, T. Luo, Y. Gao, L. Zhang, X. Huang, C. Hou, E. Long, Comparative analysis on thermal performance of different wall insulation forms under the air-conditioning intermittent operation in summer, Appl. Therm. Eng. 130 (2018) 429–438, https://doi.org/10.1016/j.applthermaleng.2017.11.042.

[17] Y. Zhang, Q. Chen, Y. Zhang, X. Wang, Exploring buildings' secrets: The ideal thermophysical properties of a building's wall for energy conservation, Int. J. Heat Mass Transf. 65 (2013) 265–273, https://doi.org/10.1016/j.ijheatmasstransfer.2013.06.008.

[18] I.R. Maestre, P.R. Cubillas, L. Pérez-Lombard, Transient heat conduction in multi-layer walls: An efficient strategy for Laplace's method, Energy Build. 42 (4) (2010) 541–546, https://doi.org/10.1016/j.enbuild.2009.10.023.

[19] G. Kim, H.S. Lim, T.S. Lim, L. Schaefer, J.T. Kim, Comparative advantage of an exterior shading device in thermal performance for residential buildings, Energy Build. 46 (2012) 105–111, https://doi.org/10.1016/j.enbuild.2011.10.040.

[20] Y. Huang, J.-L. Niu, T.-M. Chung, Study on performance of energy-efficient retrofitting measures on commercial building external walls in cooling-dominant cities, Appl. Energy 103 (2013) 97–108, https://doi.org/10.1016/j.apenergy.2012.09.003.

[21] M. Shekarchian, M. Moghavvemi, B. Rismanchi, T.M.I. Mahlia, T. Olofsson, The cost benefit analysis and potential emission reduction evaluation of applying wall insulation for buildings in Malaysia, Renew. Sustain. Energy Rev. 16 (7) (2012) 4708–4718, https://doi.org/10.1016/j.rser.2012.04.045.

[22] E. Küçüktopcu, B. Cemek, A study on environmental impact of insulation thickness of poultry building walls, Energy 150 (2018) 583–590, https://doi.org/10.1016/j.energy.2018.02.153.

[23] M. Kayfeci, A. Keçebaş, E. Gedik, Determination of optimum insulation thickness of external walls with two different methods in cooling applications, Appl. Therm. Eng. 50 (1) (2013) 217–224, https://doi.org/10.1016/j.applthermaleng.2012.06.031.